ELSEVIER

Journal of Fluids and Structures 24 (2008) 1252–1261

JOURNAL OF FLUIDS AND STRUCTURES

www.elsevier.com/locate/jfs

# Simulation of the reduction of unsteadiness in a passively controlled transonic cavity flow

P. Comte[a,*], F. Daude[b], I. Mary[b]

[a]*Laboratoire d'Etudes Aérodynamiques (LEA), Université de Poitiers, ENSMA, CNRS, 43, route de l'Aerodrome, F-86036 Poitiers, France*

[b]*ONERA, 29, avenue de la Division Leclerc, 92322 Châtillon Cedex, France*

Received 10 January 2008; accepted 5 August 2008

**Abstract**

A 30 dB reduction of the peak pressure tone and a reduction by 6 dB of the background pressure found in an experiment of high-subsonic cavity flow controlled by a spanwise rod are retrieved numerically. The injection of deterministic upstream fluctuations in the large-eddy simulation (LES) domain is found to be of crucial importance, in contrast with the baseflow case. Reduction of the vortex impingement onto the aft edge of the cavity is confirmed, together with reduction of mass flow rate breathing through the grazing plane. Visual evidence of merging between the Kelvin–Helmholtz-type vortices shed downstream of the fore edge of the cavity and the von Kármán vortices shed behind the cylinder is provided. Shocklets downstream of the cylinder are also observed.


## 1. Introduction

The high levels of pressure fluctuations caused by compressible flows over open cavities have motivated considerable efforts, in order to understand the underlying physical mechanisms and develop control strategies which are effective not only for a specific design point but also for a sufficiently wide range of parameters around it to be of practical interest.

It is well established that grazing flows over open cavities, namely, cavities too short for the recirculation zone past the upstream edge to close, develop unsteadiness due to some coupling between the reattachment region near the aft edge and the region where the incoming boundary layer detaches, past the upstream edge [see e.g. Rockwell et al. (2003), Oshkai et al. (2005)]. Conceptual models developing self-sustained oscillations exist in the incompressible limit (Howe, 1997), featuring Biot–Savart-type instantaneous interaction. Pressure tones are found, the frequencies of which scale on the inverse of the cavity length $L$, and which are enharmonic up to an end correction $\gamma$ as customary in impinging flows (Powell, 1961; Rockwell and Naudascher, 1979). These models can be extended to weakly compressible flows, as in Chatellier et al. (2004). At higher Mach number, the propagative nature of the coupling has to be taken into account. The interaction is referred to as "fluid–acoustic mode" in Rockwell and Naudascher (1979), in contrast with the "fluid–fluid mode" that prevails at vanishing Mach number. Assuming that the frequency of shedding of the Kelvin–Helmholtz vortices matches that of acoustic waves propagating upstream within the cavity yields the Rossiter

*Corresponding author.
*E-mail address:* pierre.comte@lea.univ-poitiers.fr (P. Comte).

0889-9746/$ - see front matter © 2008 Elsevier Ltd. All rights reserved.
doi:10.1016/j.jfluidstructs.2008.08.001

model $f_n = (U_\infty/L)[(n-\gamma)/(M+1/\kappa)]$, in which $M = U_\infty/a$ denotes the external Mach number and $\kappa = U_c/U_\infty$ involves an average convection speed of the Kelvin–Helmholtz vortices (Rossiter, 1964). A broad set of experimental configurations provided values for both constants $\kappa$ and $\gamma$ as a function of the length-to-depth aspect ratio $L/D$ of the cavity, and the model has proved to match quite well with frequencies of the pressure tones, up to some ad-hoc tuning of both parameters. However, attempts to reduce a universal behaviour of cavity flows have not been successful, because of the observed influence of the following parameters on the receptivity of the detached mixing layer: $L/D$, but also $L/W$, $L/\theta$ and the flow parameters $\mathrm{Re}_\theta$, $M_\infty$, the shape factor of the incoming boundary layer $H = \delta^*/\theta$ and the overall pressure level $p_{\mathrm{rms}}/q_\infty$ within the cavity (Cattafesta et al., 2003). This sensitivity not only to the level of the tones but also to the broad-band noise makes the prediction and the optimization of control strategies particularly challenging [see Cattafesta et al. (2003), Rowley and Williams (2006) for a review].

The motivation here is focussed on the assessment of the needs of numerical insight to reproduce quantitatively the unsteadiness reduction effects of a simple passive actuator, in the simplest possible high-subsonic cavity configuration: such a low aspect ratio as $L/D = 0.42$ is considered, as in Forestier et al. (2003) and Larchevêque et al. (2003) in order to minimize large-scale three-dimensional (3-D) effects. The control device considered is a spanwise cylinder placed in the upstream boundary layer, as proposed in McGrath and Shaw (1996). This was proved to reduce significantly both the tone and broad-band pressure levels, provided the diameter $d$ and its height[1] $y$ are suitably chosen. One of the key enablers for this so-called High-Frequency Tone Generator is the Reynolds number independence of the cylinder's wake Strouhal number $\mathrm{St} = fd/U_\infty \sim 0.2$. A detailed experimental investigation (Illy, 2005; Illy et al., 2004) performed at ONERA for different $L/D$, boundary layer thicknesses, and Mach numbers ranging from 0.6 to 0.78, concluded that the main parameter is the ratio $y/d$, with an optimum at $y/d = 1.2$ yielding a reduction by 30 and 6 dB of the peak tone and the overall pressure rms, respectively, and this despite the added noise of the cylinder. In contrast with the baseline case, it was found that $p_{\mathrm{rms}}$ did not increase with $M$, hence a highest efficiency found at the highest $M$ possible with the experimental facility before the onset of sonic choking effects, *viz.*, $M = 0.78$.

Here, two calculations will be compared, differing essentially in the treatment of the incoming boundary layer. The numerical details are given in the next section. The results of both calculations are compared in Section 3, in which pressure and velocity statistics are presented together with visualizations. The contribution of this investigation to the current understanding of this intriguing feedback loop will eventually be summarized.

## 2. Computational set-up

The numerical methodology employed here has been adapted from Larchevêque et al. (2003) [see also Larchevêque et al. (2004), Larchevêque (2003) for other aspect ratios], for which very good agreement with the experimental counterparts was found, in particular regarding the pressure levels and the dynamics of the phase-averaged coherent structures. In this $L/D = 0.42$ case, the overall large-scale two-dimensionality of the flow makes it possible to use 2-D URANS in the portions of the flow where the boundary layer is attached, and devote most of the computing power to the matched large-eddy simulation (LES) of a streamwise portion of the flow, in a 3-D domain of span $W_{\mathrm{num}} = L$ with periodic boundary conditions, whereas the span $W = D$ of the experimental test-section (Fig. 1) is 2.4 times as large. The Reynolds number based on the length $L$ of the cavity is $8.21 \times 10^5$, as in the experiment.

The major difficulty on the numerical side is to account for the cylinder, which is of diameter $d = 2.5$ mm, whereas the thickness of the incoming boundary layer is $\delta_{99\%} = \delta = 9.8$ mm. The thickness of the boundary layer cylinder is smaller than 0.1 mm. Turbulent boundary layers have to be gridded with a wall-normal resolution of about one wall unit. In fact, $y^+_{\mathrm{min}} \sim 2$ proved to be sufficient, either in URANS or LES. The block-structured grid shown in Fig. 2 has about $\sim 20 \times 10$ grid points, and meets the LES requirements $\Delta x^+ \sim 50$, $\Delta y^+ \sim 2$, $\Delta z^+ \sim 20$. The cavity length is discretized over about 200 meshes, and there are 250 points in the spanwise direction, with $W_{\mathrm{num}} = 20d$, that is, 5 times as much as in the incompressible cylinder wake simulations (Kravchenko and Moin, 2000). In the LES, the 3-D zone is preceded by a box of width $W_{\mathrm{num}}/5 = 4d$ replicated 5 times in the spanwise direction, and in which the incoming boundary layer and its fluctuations are generated by means of a recycling method inspired by Lund et al. (1998) and adapted to compressible RANS–LES interfacing. We are aware that this spanwise replication, motivated by CPU time considerations, could be criticized because it deprives the upstream forcing of spanwise scales significantly larger than the spanwise integral scale of the turbulence generated by a canonical wake in a turbulence-free environment. Nevertheless, $W_{\mathrm{num}}/5 = 4d$ is large enough for the dominating instabilities of the wake to develop, as in Kravchenko and Moin (2000).

[1]Here defined as in Forestier et al. (2003) and Larcheveque et al. (2003), as the clearance between the bottom of the cylinder and the wall.

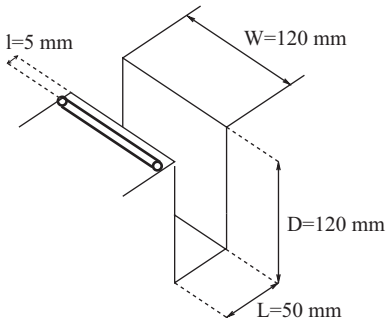


Fig. 1. Sketch of the cavity and the cylinder.

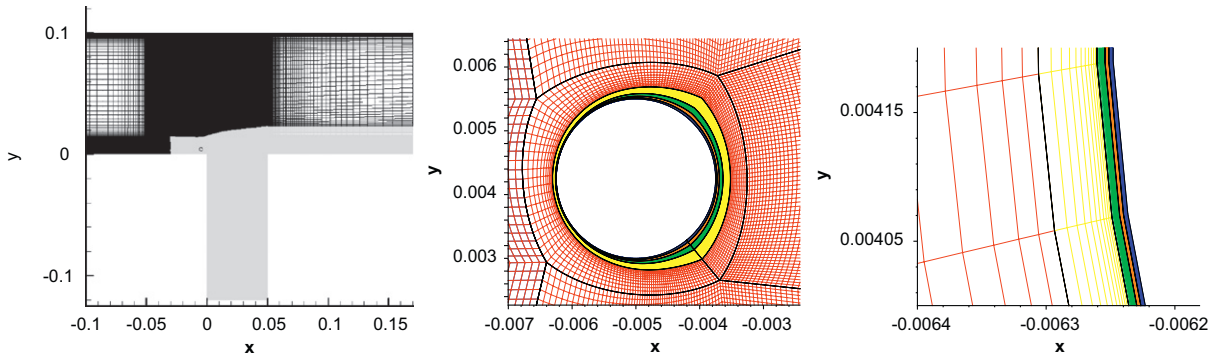


Fig. 2. Section $(x, y)$ of the grid: general view, for the LES (left). Zoom near the cylinder (middle and right, same for both calculations).

Table 1
Mesh and computational parameters for cavity simulations.

| | Number of cells ($\times 10^6$) | | | $\Delta t$ (μs) | CPU |
|---|---|---|---|---|---|
| | CFL$\leqslant$16 | CFL$\leqslant$700 | Total | | |
| LES without control | 1.6 | – | 1.6 | 1.4 | 40 |
| LES without control | 20 | 0.5 | 20.5 | 0.25 | 2200 |
| DES without control | 17 | 0.5 | 17.5 | 0.25 | 1316 |

The SubGrid-Scale model used in the LES portion (in pale shading in the left plot of Fig. 2) is the Selective Mixed-Scale model proposed in Lenormand et al. (2000). The dark regions are treated in 2-D URANS, with the Spalart–Allmaras model, as in Larchevêque et al. (2003). In that paper, the injection of realistic upstream fluctuations was not found to be needed for recovery of correct results in the baseline configuration. A repetition of it with the cylinder has thus been undertaken, with the same grid as described above, except that the region upstream of the cylinder is treated in 2-D URANS. Because it switches from URANS to LES, this calculation will be hereafter referred to as DES, although the switching is monitored by the multi-block decomposition and not by comparison between the mesh size and the local turbulence integral scale.

Implicit time integration is used, as in Larchevêque et al. (2004), but with a block-local determination of the number of iterations of the Newton-type inner process designed in such a way that the balance of the convergence errors is ensured despite the high gradient of CFL number near the cylinder. Consistency with results obtained with time-explicit schemes has been assessed in the case of the linear advection of a 2-D vortex and in the case of the low Mach number flow on an airfoil at a moderate angle of attack, near the recirculation bubble on the leeside (Daude et al., 2008).

Table 1 highlights the computational effort and the mesh size discrepancies. The CPU times mentioned correspond in each case to 50 periods of the fundamental Rossiter mode (*i.e.* 0.025 s), computed on a NEC SX6 with an average speed of 4 Gflops per processor.

## 3. Analysis of results

Fig. 3 shows the organized vortices educed by means of a positive Q surface. Both the DES and the LES develop Kelvin–Helmholtz and von Kármán-type vortices in between which streamwise vortices are stretched. The LES shows a higher level of small-scale turbulence. The corresponding movies show less large-scale unsteadiness in LES than in DES, with low-frequency flapping of the mixing layer dramatically reduced with respect to the baseline configuration, without the cylinder, which is consistent with Illy et al. (2004) and other experimental references. In particular, the impingement of spanwise-organized large-scale vortices on the aft edge of the cavity and the trapping events are visibly inhibited by the presence of the cylinder.

The pressure spectra (Fig. 4) recorded on the rear wall of the cavity at $y/D = -0.08$ show more differences between the LES and the DES than the visualizations: the LES reproduces satisfactorily the reduction of the first Rossiter mode at 2 kHz and that of the next ones observed in Illy et al. (2004). In contrast, the DES shows much less reduction of the tone levels, which shows the influence of the upstream boundary layer fluctuations. However, both calculations underestimate the peak at 20 kHz due to the wake of the cylinder, by almost 10 dB. They also underpredict the width of this peak, which is significantly wider than that of the Rossiter tones, but one should keep in mind that the pressure signal is recorded 20 diameters downstream of the cylinder, which is quite demanding in terms of resolution and numerical dissipation. Note also that the experimental pressure signal has been low-pass filtered at 30 kHz, which prevents the assessment of the numerical prediction of the high-frequency background noise. However, the latter is higher in LES than in DES, which is in agreement with the visualizations. Regarding the recycling method, the distance between the re-injection and the extraction planes would correspond, assuming advection at $U_\infty$, to a frequency of the order of 12 kHz, which does not show up on the spectra, either in LES or DES. This confirms that the recycling technique has been applied sufficiently upstream, so that the spurious correlation it introduces has enough room to decrease before it reaches the cylinder.

The effect of these upstream fluctuations is highly visible on the mean flow (Fig. 5): the recirculation length in LES is reminiscent of that of a free stream turbulent wake, whereas that in DES is about 3 times as large. This recirculation length strongly depends on the turbulence level in the boundary layer of the cylinder, which determines the position of the separation points [see Williamson (1996) for a review]. As the Reynolds number, based on the cylinder diameter, is close to $4 \times 10$, the wake would be in the subcritical regime in free stream. However, the LES yields a drag coefficient of 0.48, rather reminiscent of the supercritical regime. We however cannot be conclusive regarding the accuracy of the treatment of the boundary layer of the cylinder, and can only notice the dramatic (and beneficial) effect of the injection of deterministic upstream fluctuations. The mean streamlines show a much less pronounced upward deviation of the mean flow in LES than in DES, with about the same additional thickening of the mixing layer due to the cylinder. This was not expected *a priori*, since the deviation and thickening of the mixing layer are considered as one of the possible explanations for the tone reduction caused by the cylinder (Ukeiley et al., 2002). Notice also that the baseline configuration (right plot of Fig. 5) exhibits a small recirculation bubble, analogous to that observed at higher aspect ratio by Larchevêque et al. (2004), who emphasized its possible importance in the feedback process. Although such a bubble is not visible in either the DES or the LES, the latter shows more attached mean streamlines around the upstream edge of the cavity, which is in favour of the argument in Larchevêque et al. (2004).

The beneficial influence of the deterministic upstream perturbations is not outstandingly visible on the velocity statistics (Fig. 6). The mean velocity profiles are prescribed at $x/L = -1$ in both the DES and the LES. At $x/L = 0$, above the fore edge of the cavity, that is, $2d$ downstream of the cylinder's centreline, the turbulent kinetic energy and the Reynolds stress $u'v'$ (not shown here) in LES are correct, but the width of the wake is ever so slightly overestimated. The DES cannot build up the right turbulence level in such a short distance downstream of the cylinder. This was also the case in the DES in Arunajatesan et al. (2002). Farther downstream ($x/L = 3/5$ and $4/5$), the differences between DES and LES are less visible, but, with respect to the LDV measurements of Illy et al. (2004), the LES tends to underestimate wake diffusion, whereas the DES overpredicts it.

The presence of locally supersonic regions, too mild to educe experimentally, was suspected in Illy (2005) and Illy et al. (2004). This is confirmed, not only by the mean Mach lines shown above, but also by instantaneous snapshots and movies, as in Fig. 7. This shows, in addition to Mach contours that indicate local Mach numbers beyond 1.8, and a positive Q surface, a Schlieren-type representation of density gradient conditioned by a high value of the dilatation, in order to educe the shocklets.

The upstream part of the supersonic region is found to be relatively stable, whereas its downstream part, in which the flow decelerates causing the shocklets, oscillates at the wake shedding frequency. There is also visual evidence of merging between the Kelvin–Helmholtz-type vortices shed downstream of the fore cavity edge and the lower row of von Kármán-type vortices shed behind the cylinder. This interaction takes place either immediately around $x/L = 0$, as in

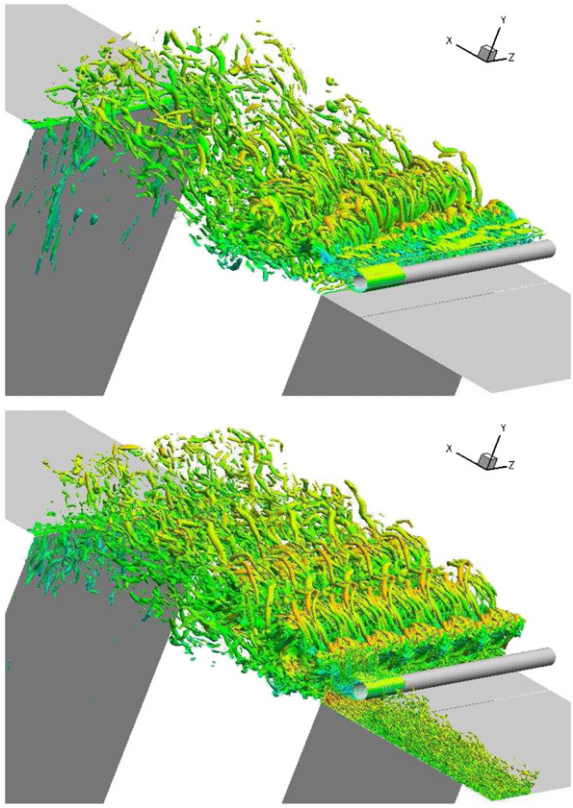

Fig. 3. Isosurfaces of $Q = 2(U_\infty/d)^2$ coloured by the streamwise velocity: DES (top), LES (bottom).

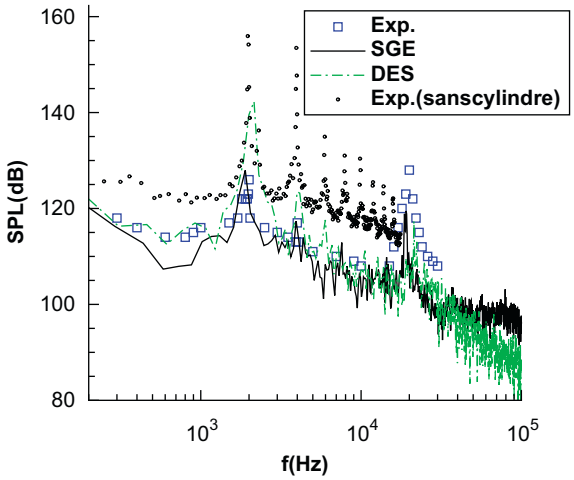


Fig. 4. Pressure spectra at the rear wall of the cavity. Dark solid line: LES; pale solid line: DES; small square symbols: baseline experiment (Forestier et al., 2003); large square symbols: controlled configuration (Illy et al., 2004).

the bottom row of Fig. 7, or farther downstream during the other alternance of the wake shedding sequence, in which case the two vortical systems can clearly be distinguished before they merge.

One of the conjectures about the tone reduction is that the cylinder wake reduces the 'breathing' of the cavity, namely, the variations of mass flow rate through its grazing plane, which is difficult to measure experimentally. This is

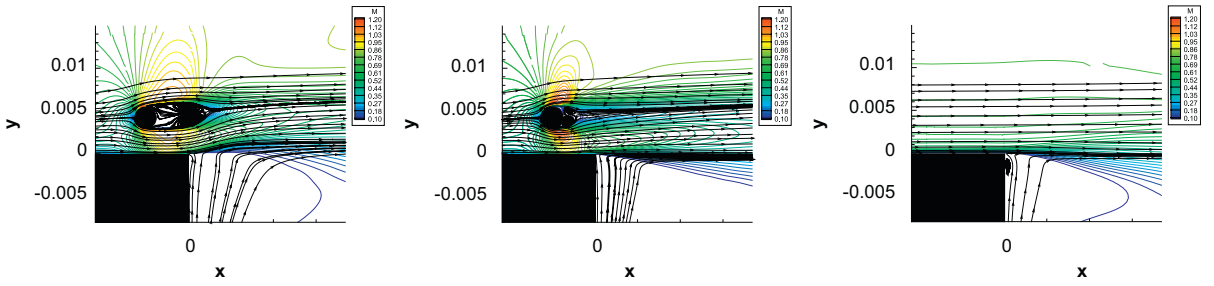


Fig. 5. Mean streamlines iso-Mach number contours in the vicinity of the cylinder: DES (left), LES (middle), baseline configuration (right).

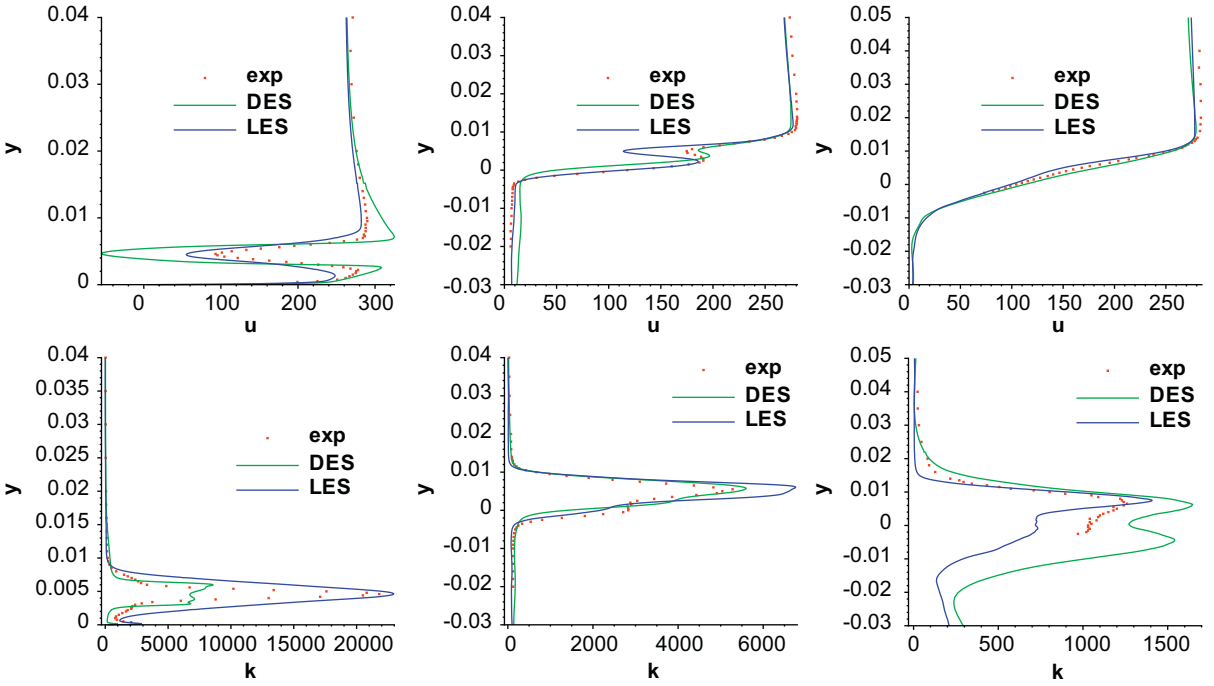


Fig. 6. Profiles at $x/L = 0$ (left), at $x/L = 1/5$ (centre) and at $x/L = 4/5$ (right). Mean velocity (top); resolved turbulent kinetic energy (bottom).

shown here in Fig. 8 from LES, in $(x, t)$ evolution after spanwise averaging (top row) and in time evolution only, after streamwise averaging (bottom row), over three periods of the fundamental Rossiter mode. In the baseline configuration, one can see about 10 in–out alternances per period near the fore edge, reduced to about 3 in the downstream quarter of the cavity, in a consistent fashion with the phase-averaged visualizations in Larchevêque et al. (2003), in which the classical 'escaped, cut or trapped' sequence was educed with outstanding agreement between numerical results and PIV measurements. With the cylinder, the breathing amplitude is reduced by a factor of about 6, with more high frequencies and more alternances in the near fore edge region, close to the cylinder. Note also a larger slope (in the $(x, t)$ representation), which suggests the reduction by about half of the convection velocity of the large-scale structures that cross the grazing plane.

Kinetic energy and pressure spectra have been recorded along 5 constant $y$ mesh lines, for 50 periods of the fundamental Rossiter mode. Its frequency corresponds to $\log(2000)\,\mathrm{Hz} = 3.3$ in Fig. 9, whereas that of the cylinder's wake is $\log(20{,}000)\,\mathrm{Hz} = 4.3$. The spectra at $y/d = 2.4$, not shown here, are very similar to those at $y/d = 1.2$ (recall that both $y$'s are symmetric with respect to the cylinder centreline), which might indicate that the near wake itself responds to the Rossiter modes: indeed, the pressure spectra at $y/d = 1.6$ show about 3 dB less peak level at $\log f = 3.3$. In any

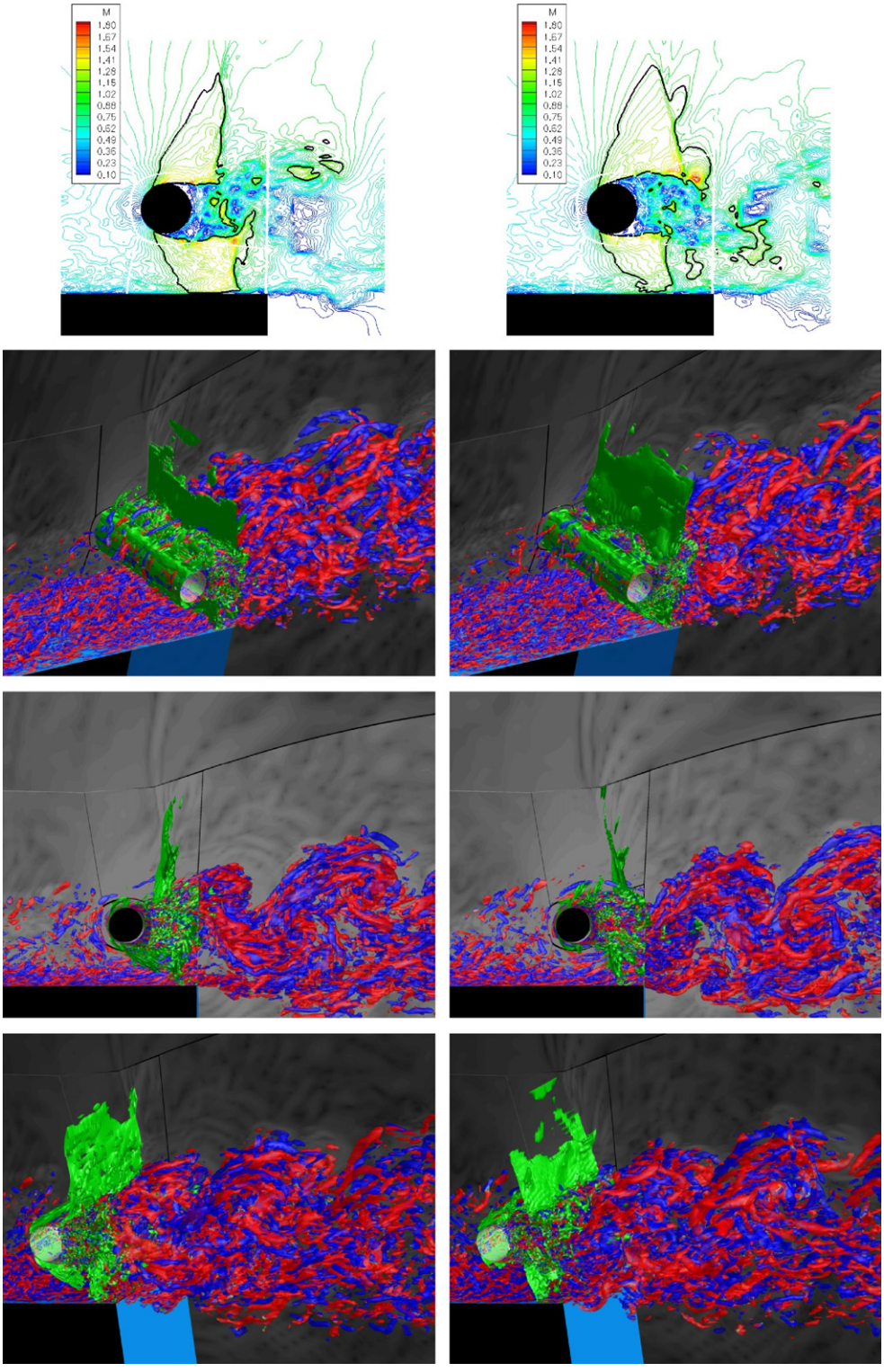


Fig. 7. Iso-Mach contours (top row, with $M = 1$ contour emphasized) and isosurfaces of $Q = 2(U_\infty/d)^2$ coloured by the streamwise vorticity (blue/red), and of $|\partial_{x\rho}\|\mathrm{div}\,\mu| = 1.3d^2/(\rho_\infty U_\infty)$ (green), at two instants of the cycle, in LES.

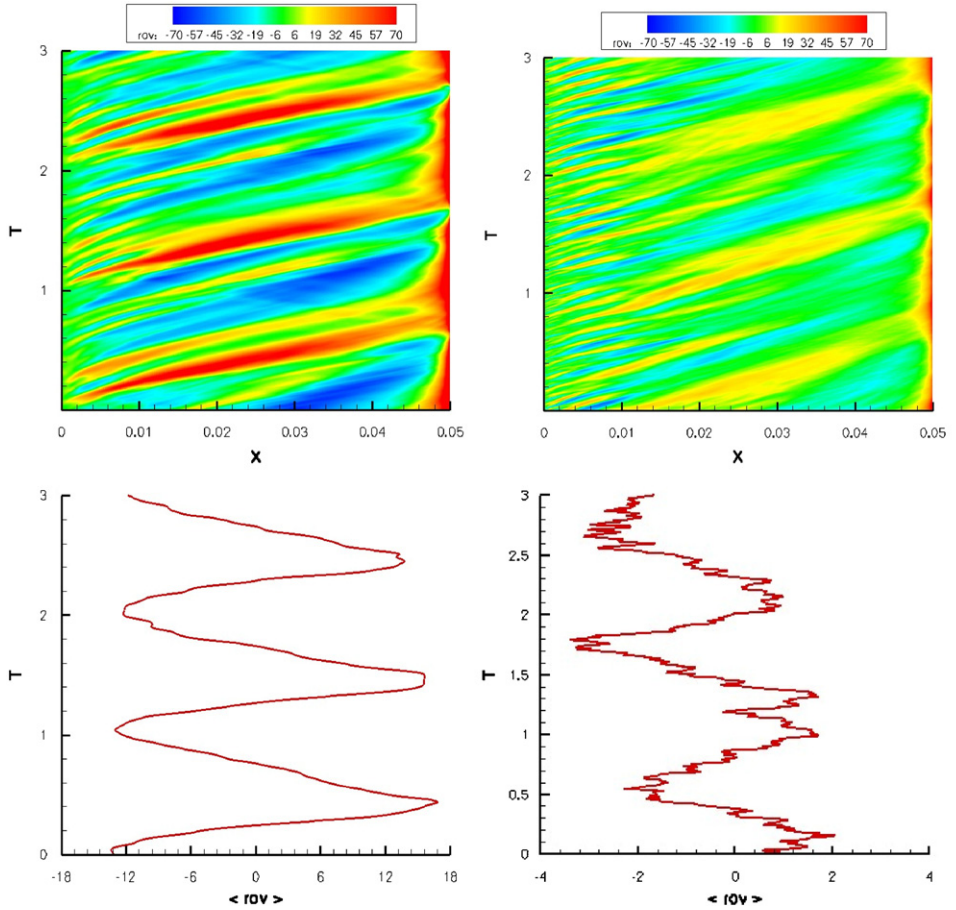


Fig. 8. Evolution of the mass flow rate through the grazing plane, Baseline configuration (left), LES with cylinder (right).

case, above the grazing plane, the pressure peaks at 20 kHz dominate those at 2 kHz, in contrast with those recorded inside the cavity (Fig. 9, right, and Fig. 4). At $y/d = 0$ and $y/d = -1.2$, we retrieve the node at $x/L = 0.5$ of the first Rossiter mode observed in Larchevêque et al. (2004) at higher aspect ratio. We also note 6 anti-nodes at 20 kHz regularly spaced along $x$, which certainly correspond to a longitudinal acoustic mode of the cavity: indeed, considering a cavity with 5 walls yields (Tam, 1976), in the absence of a flow,

$$f_{n_x,n_y,n_z} = \frac{c}{2}\left[\left(\frac{n_x}{L}\right)^2 + \left(\frac{n_x}{W}\right)^2 + \left(\frac{n_y + 1/2}{D}\right)^2\right]^{1/2}, \quad \text{hence,} \quad n_x = 2f_{n_x,0,0L}/c \sim 6.$$

## 4. Conclusion

Two hybrid RANS/LES calculations of the transonic flow over a cavity passively controlled by means of a spanwise rod are presented, and compared with the baseline configuration. The results are assessed with respect to the experimental measurements of Illy et al. (2004). With the cylinder dimensioned and position for maximal pressure tone reduction, a low $L/D$ aspect ratio is considered in order to minimize the complexity of the physics involved: in particular, the large-scale structure of the flow is quasi-2-D, which makes it possible to use spanwise periodic boundary conditions. The simulations remain nonetheless quite computationally extensive (~2000 CPU hours per run), despite the adaptation of the numerics to the grid size variations required to capture both the incoming boundary layer and that which develops on the cylinder. In contrast with the baseline case, strong sensitivity of the nature of the upstream boundary layer fluctuations is found: indeed, in the absence of deterministic forcing, the wake of the cylinder is not

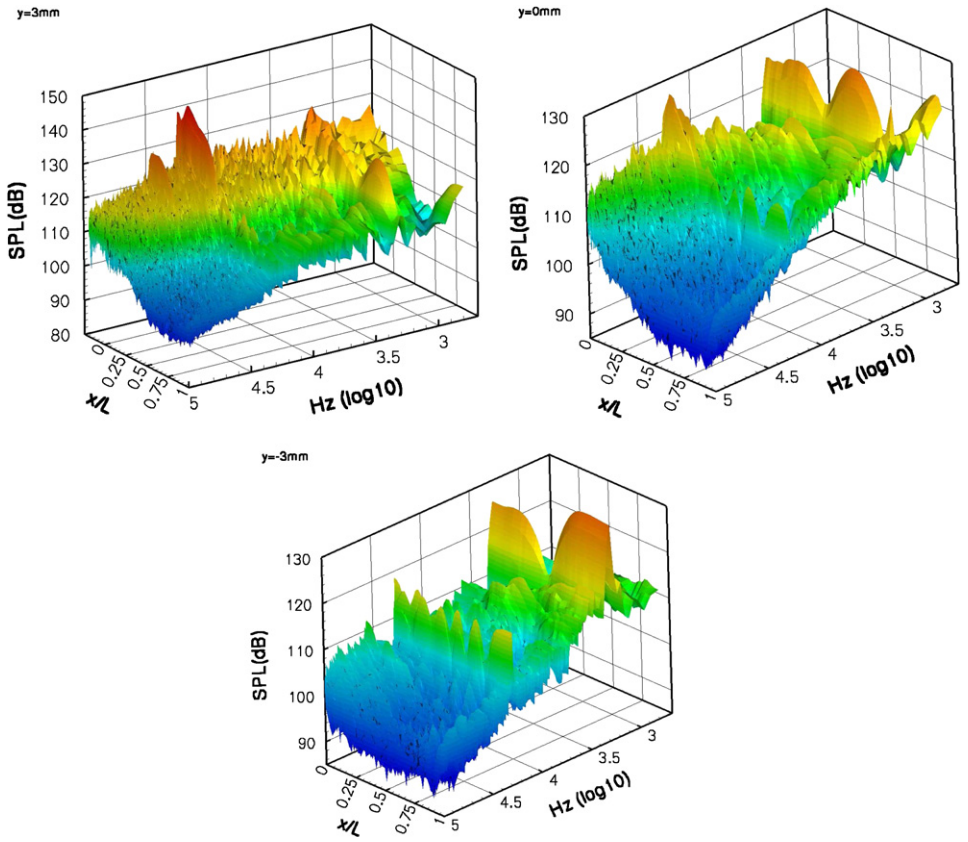


Fig. 9. Streamwise evolution of the pressure spectra at $y/d = 1.2$ (top left), $y/d = 0$ (top right) and $y/d = -1.2$ (bottom).

turbulent enough to reduce the pressure tones to the experimental level, whereas an analogous simulation with deterministic fluctuations generated by the recycling method is proved to be successful. The visualizations confirm that the impingement of Kelvin–Helmholtz-type vortices onto the aft edge of the cavity is indeed reduced, in agreement with Ukeiley et al. (2002). However, the two simulations do not show dramatic differences in the mean flow properties, and the mean upward deflection of the mean flow does not seem to be significant. Reduction of the amplitude of the mass flow rate 'breathing' through the grazing plane by a factor of 6 is observed with respect to the baseline case, together with the enrichment of the frequency content, due to additional small scales injected in the vicinity of the wake near the upstream edge of the cavity. This is in a sense consistent with the argument of Stanek et al. (2000), although analogous tone reduction effects were observed by Illy (2005) at lower frequency ratio between the fundamental Rossiter mode and the wake shedding mode, here equal to 10. Finally, evidence of shocklets is provided, which was conjectured experimentally but difficult to measure.

## References

Arunajatesan, S., Shipman, J.D., Sinha, N., 2002. Hybrid RANS–LES simulation of cavity flow fields with control. AIAA Paper 2002-1130.

Cattafesta, L., Williams, D., Rowley, C.W., Alvi, F., 2003. Review of active control of flow-induced cavity resonance. AIAA Paper 2003-3567.

Chatellier, L., Laumonier, J., Gervais, Y., 2004. Theoretical and experimental investigation of low Mach number cavity flow. Experiments in Fluids 36, 728–740.

Daude, F., Mary, I., Comte, P., 2008. Improvement of a Newton-based iteration strategy for the large-eddy simulation of compressible flows. Journal of Computational Physics, submitted for publication.

Forestier, N., Jacquin, L., Geffroy, P., 2003. The mixing layer over a deep cavity at high-subsonic speed. Journal of Fluid Mechanics 475, 101–145.

Howe, M., 1997. Edge, cavity and aperture tones at very low Mach numbers. Journal of Fluid Mechanics 330, 61–84.

Illy, H., 2005. Controle de l'ecoulement au-dessus d'une cavite en regime transsonique. Ph.D. Thesis, Ecole Centrale de Lyon.

Illy, H., Geffroy, P., Jacquin, L., 2004. Control of cavity flow by means of a spanwise cylinder. In: 21st ICTAM, Warsaw.

Kravchenko, A.G., Moin, P., 2000. Numerical studies of flow over a circular cylinder at $Re_D = 3900$. Physics of Fluids 12 (2), 403–417.

Larchevêque, L., 2003. Simulation des grandes echelles de l'ecoulement au-dessus d'une cavite. Ph.D. Thesis, Universite de Paris Vl-Pierre et Marie Curie.

Larchevêque, L., Sagaut, P., Mary, I., Labbe, O., Comte, P., 2003. Large-eddy simulation of a compressible flow past a deep cavity. Physics of Fluids 15 (1), 193–210.

Larchevêque, L., Sagaut, P., Le, T.-H., Comte, P., 2004. Large-eddy simulation of a compressible flow in three-dimensional open cavity at high Reynolds number. Journal of Fluid Mechanics 516, 265–301.

Lenormand, E., Sagaut, P., Ta Phuoc, L., Comte, P., 2000. Subgrid-scale models for large-eddy simulation of compressible wall bounded flows. AIAA Journal 38 (8), 1340–1350.

Lund, T.S., Wu, X., Squires, K.D., 1998. Generation of turbulent inflow data for spatially-developing boundary layer simulations. Journal of Computational Physics 140 (2), 233–258.

McGrath, S.F., Shaw, L.L., 1996. Active control of shallow cavity acoustic resonance. AIAA Paper 96-1949.

Oshkai, P., Geveci, M., Rockwell, D., Pollack, M., 2005. Imaging of acoustically coupled oscillations due to the flow past a shallow cavity: effect of a cavity length scale. Journal of Fluids and Structures 20, 277–308.

Powell, A., 1961. On the edgetone. Journal of the Acoustic Society of America 33, 395–409.

Rockwell, D., Naudascher, E., 1979. Self-sustained oscillations of impinging free shear layer. Annual Review of Fluid Mechanics 11, 67–94.

Rockwell, D., Lin, J.C., Oshkai, P., Reiss, M., Pollack, M., 2003. Shallow cavity flow tone experiments: onset of locked-on states. Journal of Fluids and Structures 17, 381–414.

Rossiter, J.E., 1964. Wind-tunnel experiments on the flow over rectangular cavities at subsonic and transonic speeds. Aeronautical Research Council Reports and Memoranda 3438.

Rowley, C.W., Williams, D.R., 2006. Dynamics and control of high Reynolds-number flow over open cavities. Annual Review of Fluid Mechanics 38, 251–276.

Stanek, M.J., Raman, C., Kibens, V., Ross, J.A., Odedra, J., Peto, J.W., 2000. Control of cavity resonance through very high frequency forcing. AIAA Paper 2000-1905.

Tam, C.K.W., 1976. The acoustic modes of a two-dimensional rectangular cavity. Journal of Sound and Vibration 49 (3), 353–364.

Ukeiley, L.S., Ponton, M.K., Seiner, J.M., Jansen, B., 2002. Suppression of pressure loads in cavity flows. AIAA Paper 2002-0661.

Williamson, C.H.K., 1996. Vortex dynamics in the cylinder wake. Annual Review of Fluid Mechanics 28, 477–539.